

Application of Energy Storage Elements on a PV System in the Smart Grid Context

Filipe Perez, Júlio Freitas Custódio, Vitor Grillo de Souza, Homero Krauss Ribeiro Filho, Edison Massao Motoki, Paulo

Fernando Ribeiro

CERIn – Centro de Excelência em Redes Elétricas

UNIFEI – Universidade Federal de Itajubá

Itajubá, Brazil

filipe.perez@unifei.edu.br, julio.custodio@unifei.edu.br, homerokrauss@yahoo.com.br, pvgrillo@hotmail.com,

edison.motoki@unifei.edu.br, pfribeiro@ieee.org

Abstract— The use of renewable resources, such as solar energy, in distributed generation can bring instabilities to the system due to fluctuations in power output caused by variations or bad weather. In order to reduce the impacts caused by solar panels (PV's), the application of intelligent networks is feasible to control the distributed generation. Inserting storage energy elements in PV's stabilizes the energy produced by the panel, very sensitive to temperature and solar irradiation. In this context, we developed a computational model of 100 kW photovoltaic systems connected to the network with storage elements for the uniform supply of power, which has a load control strategy and battery discharge, standardizing the power delivery network. Therefore, it was verified the importance of smart grids in the control of power flow.

Index Terms— Distributed generation, Storage energy, Smart grid, Photovoltaic systems, Power flow control.

I. INTRODUCTION

The distributed generation through photovoltaic (PV's) has been widely applied, especially in Europe to expand and diversify its energy matrix due to the finite nature of fossil fuels, and aiming at the generation of clean energy, with the lowest level of environmental degradation [1].

The photovoltaic systems are suitable for installation in any location where there is a high incidence of solar radiation. Due to this fact, Brazil has a great energy potential for the PV plant. This system can be easily adapted in the buildings architecture and can be installed in facades, roofs and walls of buildings, homes, country houses and several other buildings [2].

The use of solar energy through photovoltaic cells has been characterized by the installation of small power sources distributed throughout the network. There are great incentives and subsidies for the installation of alternative energy resources by the ongoing concern with environment preservation [3].

By 2012, it has been installed 102 GW in photovoltaic systems worldwide, and 95% of these were connected to the network. With an output at this level it can be saved 52 million

tons of CO₂, which it would be released into the atmosphere, by thermal power plants and nuclear reactors. The trend is that the installed solar power generation becomes increasingly larger. A pessimistic forecast based by the members of industry, government agencies and electric utilities, estimates that the growth in power generated added on 48 GW in 2017, and in a scenario driven by political incentives, the increase could reach 84 GW installed worldwide in 2017. The Figure 1 shows the growth of the power of photovoltaic panels installed on the network [4].

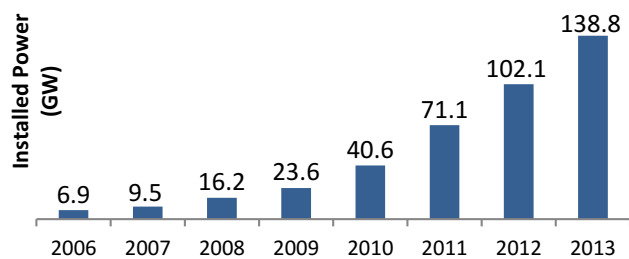


Figure 1. Growth of solar panels installed by 2013.

The great problem of distributed generation through renewable resources is the dependence on natural sources, which have many uncertainties and variations. Solar generation is at the mercy of bad weather, which often brings clouds or storms that generate shading and temperature change, impacting directly in the production of electricity. Therefore, it becomes a necessity the usage of elements to store excess of energy to regulate the power that is injected into the network [5].

The battery bank is a very important element in distributed generation when referring to the power flow control, it allows the energy produced by the panel be delivered to the grid more constant and in a balanced way, avoiding large drops in supply power, caused by shading and temperature change on the panel. The energy storage element may represent about 15% of the initial installation costs, reaching 46% if considered maintenance costs. This is explained by the fact that the battery

lifecycle is smaller than the other components of the photovoltaic system [6].

In addition, the batteries are subjected to various operating conditions, due to the behavior of non-linear panels. There are several models of batteries available in the market, but this work will only use the lithium ions, which have some advantages listed below: higher storage capacity than the others; allows to be charged several times a day; absence of memory effect; long life cycle; low maintenance; less toxic than other models; higher energy density. However, this type of battery has a high cost, high risk of damage overload, self-discharges and risk of explosion if there is no adequate control of the temperature [6-8].

In this context, the load control method aims to boost the lifetime of the batteries, considering the state of charge, nominal current, voltage fluctuation and the battery temperature. At the time of discharge, the battery must not exceed the nominal discharge current, which characterizes its ability to withstand deep discharge. In charge mode the battery must not exceed the maximum voltage level allowed by the manufacturer, as this could cause dilation and increase the risk of explosions [9].

The application of storage energy elements along with photovoltaic panels in the context of smart grid offers a valuable condition for the power flow control of a system, eliminating the power fluctuations on the network. As a result, it allows an improvement in the quality of energy in a situation of distributed generation and micro-grids [5, 10].

II. PHOTOVOLTAIC PANEL

The equation of a PV is described in (1),

$$I = I_{pv} - I_0 \left(e^{V + I R_{sm} / a k T} - 1 \right) - \frac{V + I R_{sm}}{R_{pm}} \quad (1)$$

where I_{pv} and I_0 can be calculated in (2) and (3) respectively:

$$I_{pv} = (I_{pv_n} + K_i \Delta T) \frac{G}{G_{ref}} \quad (2)$$

$$I_0 = \frac{I_{sc_n} + K_i \Delta T}{e^{(V_{oc_n} + K_v \Delta T) / a k T} - 1} \quad (3)$$

In nominal conditions I_{pv_n} can be calculated by,

$$I_{pv_n} = \frac{R_{pm} + R_{sm}}{R_{pm}} I_{sc_n} \quad (4)$$

where I_{pv} is the current generated in the semiconductor panel, I_0 is the reverse current of the diode, G and G_{ref} are the irradiation incident and the reference irradiation, respectively. $\Delta T = T - T_n$, where T is the temperature in the panel and T_n is the ambient temperature, K_i is the temperature coefficient of short-circuit current I_{sc} . So, I_{sc_n} and V_{sc_n} are the nominal voltage and current in PV respectively, a is the diode ideality factor, k is the Boltzmann constant, R_{sm} represents the losses by falling voltage for the current flowing to the load, R_{pm} is the reverse leakage current of the diode and V_{oc} represents the voltage drop across the diode. The resistors shown may be

estimated on the basis of the parameters provided by the manufacturer [11, 12].

The electric model of PV is represented in Figure 2.

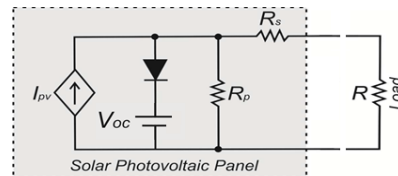


Figure 2. The electric model of PV.

The Figure 2 displays a PV containing 5 modules in series and 66 modules in parallel, which generates 100 kW at maximum power, with a voltage of 273.5 V. It is presented in Table I the parameters of panel at 25°C of temperature and 1000 W/m² solar radiation, which are the normal conditions of a PV.

The Figure 3 shows the characteristic curves of the panel where it is indicated that, for each value of temperature and solar radiation, there is a point of maximum power P_{max} , related to voltage V_{mp} and maximum output current I_{mp} shown in Table I in nominal conditions of the PV [13].

TABLE I. PARAMETERS OF SOLAR PANEL

| Parameter | Value |
|--|----------|
| Number of Cells per Module | 96 |
| Maximum Power, P_{max} (W) | 300 |
| Maximum Power Voltage, V_{mp} (V) | 54,7 |
| Maximum Power Current, I_{mp} (A) | 5,58 |
| Open-Circuit Voltage, V_{oc} (V) | 64,2 |
| Short-Circuit Voltage, V_{sc} (A) | 5,96 |
| Temperature Coefficient of V_{oc} (V/K) | -0,177 |
| Temperature Coefficient of I_{sc} (A/K) | 0,003516 |
| Temperature Coefficient of V_{mp} (V/K) | -0,186 |
| Temperature Coefficient of I_{mp} (A/K) | -0,00212 |
| Diode Ideality factor, a | 1,25 |
| Series Resistance, R_{sm} (Ω) | 0,0830 |
| Parallel Resistance, R_{pm} (Ω) | 819,13 |

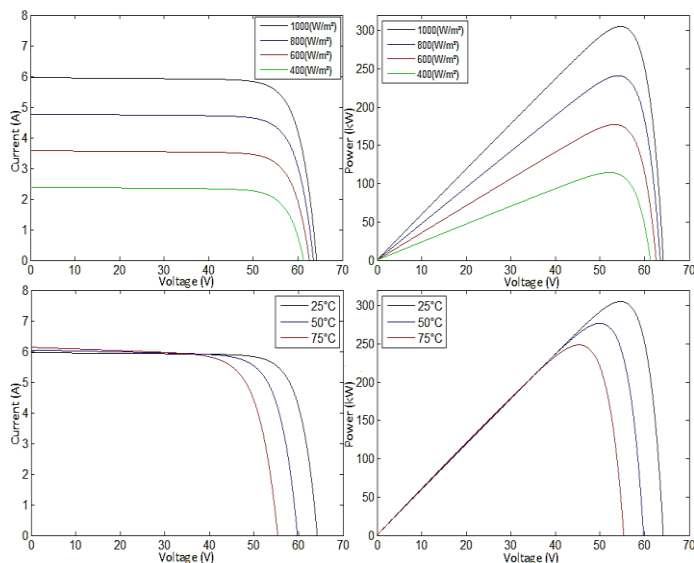


Figure 3. Characteristic curves of PV.

III. BATTERY BANK

The mathematical model of the battery is represented by different equations for the charge and discharge mode. Thus (5) and (6) are the equations for the discharge and charge mode, respectively [14].

$$V_{bat} = V_0 - Ri - K \frac{Q}{Q-it} (it + t^*) + e^t \quad \square 5$$

$$V_{bat} = V_0 - Ri - \left(K \frac{Q}{it-0,1Q} \right) i^* - \left(K \frac{Q}{Q-it} \right) it + e^t \quad \square 6$$

where V_{bat} is the instantaneous voltage of the battery, V_0 is the rated voltage, K is the resistance of polarization or open circuit voltage (V/Ah), Q is the rated capacity, A is the exponential zone, $it = \int idt$ which is the instantaneous load, B is the inverse exponential time zone (Ah^{-1}), R is the internal resistance, i is the current in the battery and i^* is the current filtered battery [15]. The battery is designed to supply a power of 240 kW for the period of time if the panel fails or sunlight approaches zero [5]. The Table II shows the data of a lithium ion.

TABLE II. PARAMETERS OF STORAGE ENERGY ELEMENT

| Parameter | Value |
|----------------------------------|-----------|
| Nominal Voltage (V) | 120 |
| Nominal Capacity (Ah) | 2000 |
| State of Charge (%) | 50 |
| Maximum Capacity (Ah) | 2153,8462 |
| Voltage Full Charge (V) | 141,3559 |
| Nominal Current Discharge (A) | 869,5652 |
| Internal Resistance (Ω) | 0,0006 |

IV. COMPUTER MODEL SETUP

The intelligent network model proposed has a set of PV's totaling 100 kW in nominal conditions in parallel to a battery bank of 48 kW connected in the DC link of a three-phase inverter which injects power to the grid, and set some charges in the system which will be detailed later. The model is shown in Figure 4.

The purpose is to analyze the integration model of distributed generation connected to the network. Therefore, it is implemented models of chokes representing transmission lines and loads connected to the network. The voltage generated by the PV need of converters (VSC's) to be integrated, which may cause pollution to the network in the form of harmonic distortion. It takes two stages of static converters, where in the first converter is set to control the voltage and current generated in the panel. The boost converter is used for this purpose, which is characterized by the amplification of the output signal [16].

The second conversion stage is to transform the voltage generated in the panel, which is made by the VSC. The VSC converts the output voltage of the boost converter, which is continuous in a three-phase AC voltage, which thus may be delivered to the network. The network provides the reference of voltage and current for the VSC in order to achieve synchronism and parallelism with the grid, so that the generated power can be consumed. The input voltage of the converter forms the DC link, which is a point in common between the converters panel and battery. The voltage in this point of the

system should be controlled to remain constant for the correct function of the system.

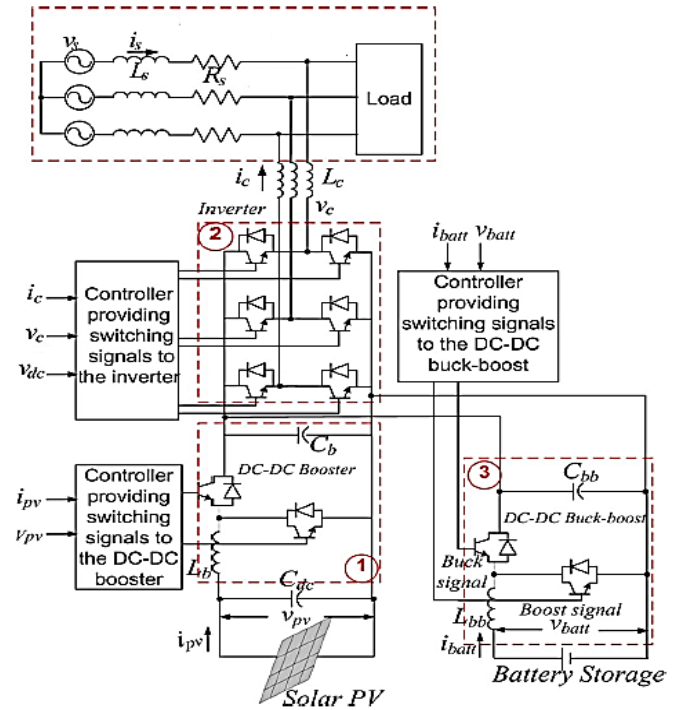


Figure 4. PV control configuration, the battery bank and inverter.

Another converter used is a bidirectional boost converter, used to control the power flow storage bank, that is, it allows injection and power absorption in the battery. The converter acts as buck in network power absorption when the battery is charged and as a boost when the battery performs a discharge. In this case, the battery current needs to be controlled, due to the fact that it may take positive and negative values by following the controller signal [14].

In Table III, Table IV and Table V, are shown the parameters of the converters which were used in the model.

TABLE III. PV'S BOOST CONVERTER PARAMETERS

| Parameter | Value |
|----------------------------------|--------|
| Inductor Inductance (mH) | 5,0 |
| Inductor resistance (Ω) | 0,005 |
| Input Capacitor (μF) | 100 |
| Resistance of IGBT (Ω) | 0,001 |
| Frequency Switching (kHz) | 5 |
| Conduct Voltage IGBT (V) | 0 |
| Diode Resistance (Ω) | 0,0001 |
| Diode Conduct Voltage (V) | 0 |

TABLE IV. BIDIRECTIONAL BOOST CONVERTER PARAMETERS

| Parameter | Value |
|----------------------------------|-------|
| Inductor Inductance(mH) | 8,0 |
| Inductor resistance (Ω) | 0,001 |
| Input Capacitor (μF) | 12 |
| Resistance do IGBT (Ω) | 0,001 |
| Frequency Switching (kHz) | 10 |
| Conduct Voltage IGBT (V) | 1 |
| Diode Resistance (Ω) | 0,001 |
| Diode Conduct Voltage (V) | 0,8 |

TABLE V. VSC CONVERTER PARAMETERS

| Parameter | Value |
|--|----------|
| Number of arms | 3 |
| Resistance of Snubber (M Ω) | 1 |
| Capacitance of Snubber (F) | ∞ |
| Internal Resistance of IGBT (Ω) | 0,0002 |
| Frequency Switching (kHz) | 1,98 |
| Conduct Voltage IGBT (V) | 0 |
| Device Conduct Voltage (V) | 0 |

A. Maximum Power Point Tracker (MPPT)

The control on the PV is done through a MPPT algorithm that maintains the panel at maximum power point at all levels of solar radiation and temperature changes. The algorithm used in the model is the incremental conductance, which has a quicker response compared to other known algorithms. In this method, the maximum power is obtained when the derivative of power in relation to voltage is equal to zero. The Figure 5 shows an illustration of this algorithm.

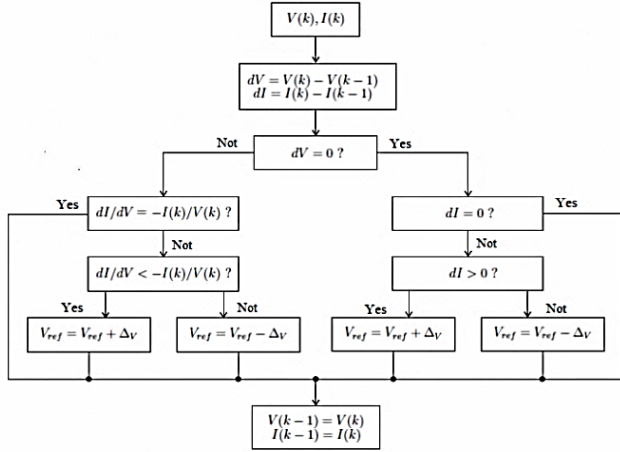


Figure 5. Incremental conductance algorithm [12].

The algorithm generates an input reference to control the boost converter and from this reference generates a signal that is applied to the converter that controls the panel at full power.

B. Battery Bank Control

The bidirectional boost converter conducts the power flow of the system according to the power generated in panel P_{pv} . It is desired that the power flow for the network is constant at 80kW, regardless of variations in the panel. So the battery should complement the power supply when the PV does not supply enough. If $P_{pv} > 80$ kW, then the battery absorbs surplus power to be charged, but if $P_{pv} < 80$ kW, the battery injects power into the system to regulate the generation. The Figure 6 shows how the signal is generated in the battery converter.

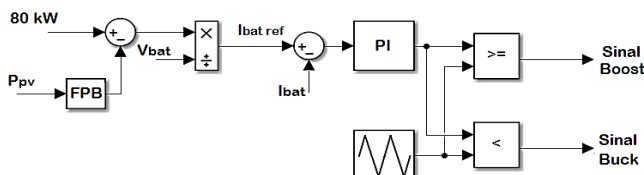


Figure 6. Power control diagram in the battery.

C. Frequency Inverter Control

The frequency inverter controls the voltage in the DC link, set at 500 V. When the generated power increases, the voltage on the DC link rises and when the generation in PV decreases, the voltage drops. Then it is possible to detect variations of generation in the system and control the power flow. The PWM signal generated in the inverter is obtained by comparing the triangular wave with three signals: the phase voltage network V_c , line current I_c and output voltage of the boost V_{dc} . As a result, the converter performs the control of the network power injection. The Figure 7 shows the VSC control method.

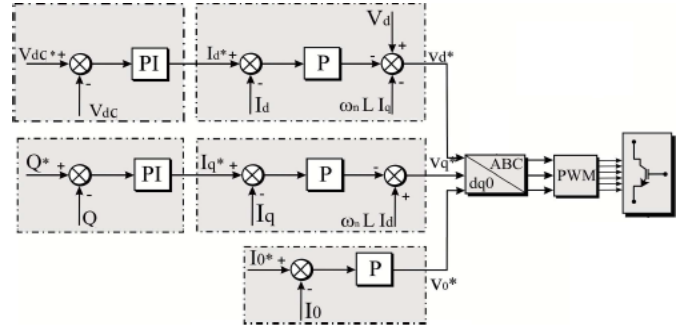


Figure 7. VSC control diagram.

V. APPLICATION EXAMPLE

It was developed in Matlab/Simulink a photovoltaic system in parallel with a storage element, which is integrated into the network via an inverter. The MPPT controller uses the incremental conductance control algorithm with a switching frequency of 10 kHz. The inverter has a switching frequency of 1,98 kHz, and the DC link voltage is 500 V three-phase output of 260 V and 60Hz.

Therefore, the generated voltage passes through an LC filter with an 250uH inductor and a capacitor of 10 kVAR to filter the harmonics generated by the inverter. A transformer of 100 kVA transforms the voltage in relation of 160V/25kV, representing a distribution system where the PV is inserted. The simulated network has a line of 21 km with its own chokes. There is a resistive load of 2 MW and an inductive load of 30 MW and 2 MVAR at the end of the line.

A grounding transformer is also added to the end of the line in order to protect the system. The grounding resistance is 3,3 (Ω), the transformer has a zero sequence impedance of 0,025 + 0,75j (Ω) pu, and its nominal power is 100 MVA. The distribution system is connected to the transmission line by a 47 MVA transformer to high voltage with relationship of 25kV/120kV and the network has a short circuit power of 2500 MVA, which complements the existing power loads on the system. The simulated values reflect real values, which can be applied in a real electrical system.

The bidirectional converter connected to the battery has IGBT's that allows the current flows in both directions, allowing the battery to make loading and unloading cycles. Therefore, in fact the converter does not work at any time in discontinuous conduction regime.

The Figure 8 shows the input signal of the panel, solar irradiation and temperature. The variations characterize shades,

risers in temperature, or even a panel failure. These variations have similar characteristics to reality, allowing to observe the system control dynamics.

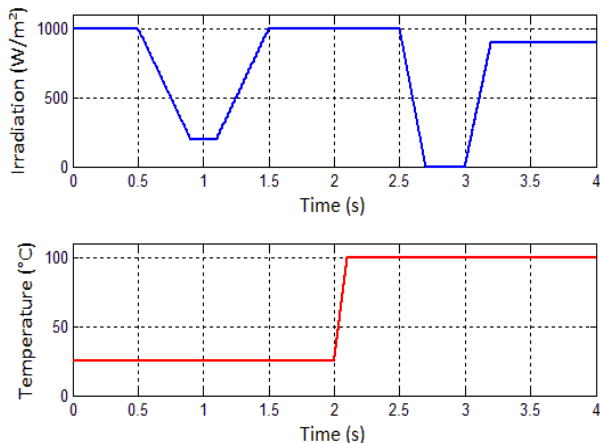


Figure 8. Input parameters in PV.

A. Results and Analysis

The PV is controlled at full power, so the MPPT appears to be quite functional because it can maintain maximum power, even with the irradiation and temperature oscillations. In nominal conditions, the PV generates 100 kW at 25°C and 70 kW at 100°C. It can be observed the MPPT control in dynamic voltage and current of the panel in Figure 10, which has few fluctuations and rapid response. In Figure 11 it is possible to perceive the battery voltage, which remains constant as expected and the current control acting to make necessary changes in battery current to maintain constant power flow to the network, which in fact can be seen in Figure 9, which shows the sum of the power generated by the panel with the battery.

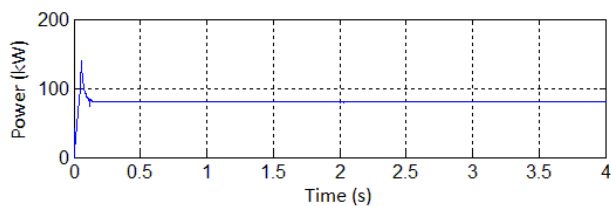


Figure 9. Power delivered to grid.

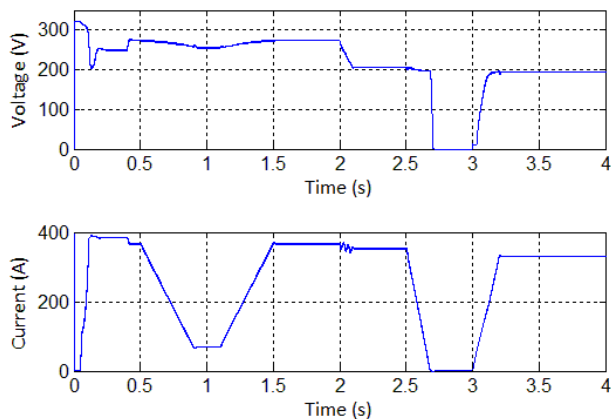


Figure 10. Voltage and current controlled in PV.

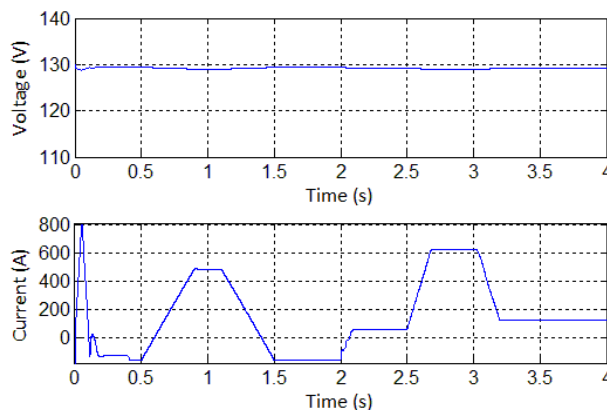


Figure 11. Voltage and current of the battery controlled by bidirectional boost.

The Figure 12 shows the power generated in the power panel and the battery bank which varies exactly in accordance with the variations of the power generated in the panel. It can be seen that at two times the power in the battery is negative, which indicates that the battery absorbs the power generated in the panel precisely to regulate the power flow in the system. In Figure 13 is shown the voltage and current in pu after the transformer. It is observed the voltage stability, and the minor variations in current of loads, which are due to the changes originated from the PV.

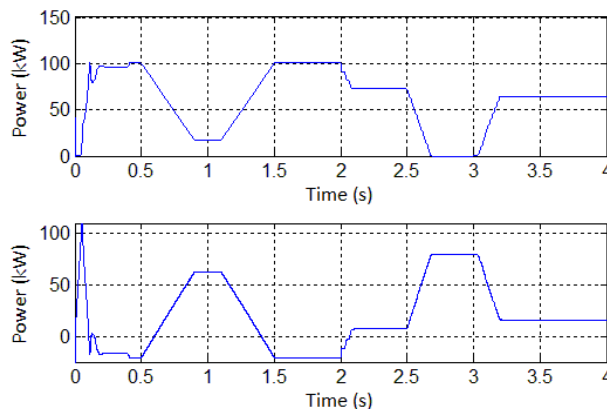


Figure 12. Power generated by the PV and the power in the battery bank.

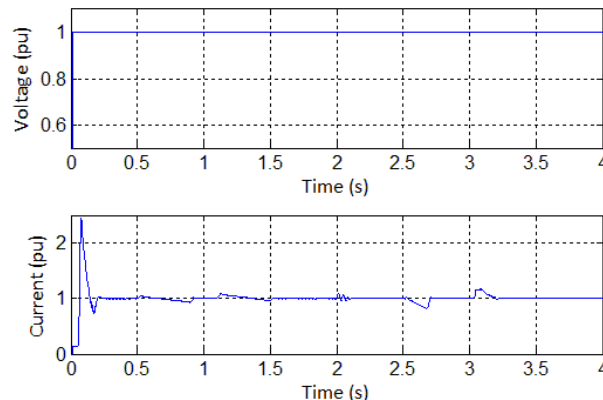


Figure 13. Voltage and current in p.u. load.

In Figure 14, it can be seen that the control on the DC link generates some disturbances in the power delivered to the grid,

as it enters the dynamic control of the containing element. Yet it is shown in Figure 14 that the output power of 20 kV transformer is slightly below 80 kW originally desired, but this is due to losses in the system elements, transformer, inverters, and resistances in the transmission lines.

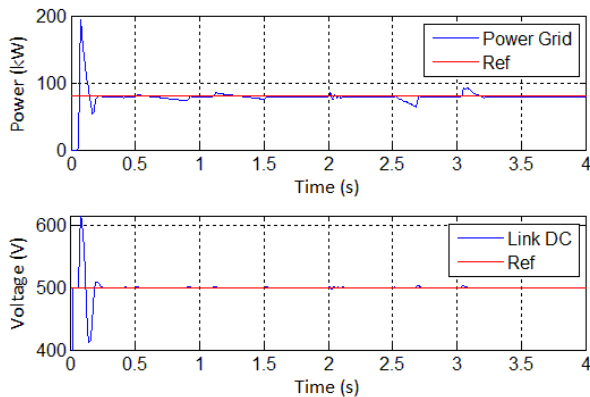


Figure 14. Power transformer and voltage in the DC link.

B. Harmonic Distortion Analysis

In the case of a distributed generation using a three-arm converter with low switching frequency of 1,98 kHz, the use of filters is required so that the levels of harmonic distortion remain within the recommendations of the IEEE-519. Thus, the system can be connected into the network according to regulatory norms of each country.

The Table VI shows the levels of harmonic distortion generated by the photovoltaic system when there is no filter, as well as the levels of harmonics after filtering according to the recommendations of IEEE-519 [17].

| Parameter | THD Current | THD Voltage |
|---------------------|-------------|-------------|
| Without Filter | 6,45% | 41,20% |
| With Filter | 0,26% | 0,28% |
| IEEE Recommendation | < 5,00% | < 5,00% |

According to Table VI, it is possible to notice that there is a great distortion in the generated voltage over the established limit, which occurs mainly by the three-phase converter, on the other hand, the filter is efficient. Eliminating the harmonic distortions, leaving the THD current, THD voltage and even all the individual harmonics fit within the recommendations [17]. This in fact guarantees the proper functioning of the system.

VI. CONCLUSIONS

This article proposed a modeling and complete simulation of photovoltaic systems with storage energy element in smart-grid context for power flow analysis system, in order to minimize the power generated from fluctuations in PV's which are caused by climate oscillations over a period of the day.

Smart grids help to improve the reliability and stability of electrical systems, as in the photovoltaic generation system allows good stability and power flow control. Note that Brazil has great potential for photovoltaic generation, and this

alternative generation resource should be encouraged in the context of distributed generation.

In the full computer simulation (electrical system and controls) was possible to keep the generation of PV 80 kW continuously as proposed by minimizing the impacts of intermittency of solar generation. The power flow control acts in an accurate and balanced way, without overshoot and few swings even though being considered a robust system. The battery bank helps in removing fluctuations on the network, serving as a power router, absorbing the peaks of the PV generating and maintaining the power and voltages on the uniform grid.

Finally, it is recommended a more specific control of the battery, with overload and overheating protection system, and monitoring the battery charge stages.

VII. REFERENCES

- [1] M. G. Villalva, and J. R. Gazoli, "Comprehensive approach to modeling and simulation of photovoltaic arrays," *Power Electronics, IEEE Transactions on*, vol. 24, no. 5, pp. 1198-1208, 2009.
- [2] A. Montenegro, A. S. A. C. Diniz, A. C. d. M. Junior, E. S. Lousada, E. F. d. Medeiros, J. B. Xavier, H. M. Schneider, I. Zanesco, M. L. Pomper Mayer, P. Malamud, R. D. Filho, and R. G. Araújo, *Estudo e Propostas de Utilização de Geração Fotovoltaica conectada à rede, em Particular Edificações Urbanas*, Ministério de Minas e Energia, 2009.
- [3] E. d. P. Energética, "Aspectos Elétricos e Energéticos - Geração Fotovoltaica," *Revista Ecoenergia*, 2014.
- [4] E. P. I. Association, "Global market outlook for photovoltaics until 2014," http://www.epia.org/fileadmin/EPiA_docs/public/Global_Market_Outlook_for_Photovoltaics_until_2014, 2010.
- [5] Z. Wang, X. Li, G. Li, M. Zhou, and K. Lo, "Energy storage control for the Photovoltaic generation system in a micro-grid." pp. 1-5.
- [6] V. E. Neto, F. Perez, A. G. Tôres, A. F. Cupertino, and H. A. Pereira, "Passivity-Based Control for Charging Batteries in Photovoltaic Systems."
- [7] R. P. Lima, "Monitoramento da Descarga de Bateria com Uso de Microprocessador," Universidade Federal do Rio de Janeiro, 2012.
- [8] E. W. Santos, and R. S. Matsumoto, "DIBB-Dimensionador de banco de baterias."
- [9] P. E. M. Pellegrino, "Dimensionamento de Baterias," 2006.
- [10] Y. Wang, X. Lin, and M. Pedram, "Adaptive Control for Energy Storage Systems in Households With Photovoltaic Modules," *IEEE Trans. Smart Grid*, vol. 5, no. 2, pp. 992-1001, 2014.
- [11] A. Cupertino, J. de Resende, H. Pereira, and S. S. Júnior, "A Grid-Connected Photovoltaic System with a Maximum Power Point Tracker using Passivity-Based Control applied in a Boost Converter," the solar system, vol. 4, no. 5, pp. 6, 2012.
- [12] M. Villalva, "Conversor eletrônico de potência trifásico para sistema fotovoltaico conectado à rede elétrica," UNICAMP. Campinas, pp. 292, 2010.
- [13] R. Sankarganesh, and S. Thangavel, "Maximum power point tracking in PV system using intelligence based P&O technique and hybrid cuk converter." pp. 429-436.
- [14] A. A. Akhil, G. Huff, A. B. Currier, B. C. Kaun, D. M. Rastler, S. B. Chen, A. L. Cotter, D. T. Bradshaw, and W. D. Gauntlett, "DOE/EPRI 2013 electricity storage handbook in collaboration with NRECA," ed: Albuquerque, NM: Sandia National Laboratories, 2013.
- [15] S. Adhikari, and F. Li, "Coordinated Vf and PQ control of solar photovoltaic generators with MPPT and battery storage in microgrids," 2014.
- [16] A. Kalbat, "PSCAD simulation of grid-tied photovoltaic systems and Total Harmonic Distortion analysis." pp. 1-6.
- [17] "IEEE Recommended Practice and Requirements for Harmonic Control in Electric Power Systems," S. b. t. T. A. D. Committee, ed., 2014, p. 29.